Atmospheric Environment Vol. 24A, No. 9, pp. 2361–2368, 1990.
Printed in Great Britain.

0004–6981/90 $3.00 + 0.00
Pergamon Press plc

CALCULATION OF VISUAL RANGE IMPROVEMENTS FROM SO_2 EMISSION CONTROLS—I. SEMI-EMPIRICAL METHODOLOGY

PAOLO ZANNETTI,* IVAR TOMBACH† and WILLIAM BALSON‡

*IBM, Thormøhlensgate 55, Bergen High Tech Center, N-5008 Bergen, Norway, †AeroVironment Inc., 825 Myrtle Avenue, Monrovia, CA 91016, U.S.A. and ‡Decision Focus, Inc., 4984 El Camino Real, Los Altos, CA 94022, U.S.A.

(*First received* 8 *March* 1989 *and in final form* 19 *April* 1990)

Abstract—This paper, the first of a two-part series, presents a new semi-empirical methodology that allows estimation of the percentage improvements in annual average visual range that can be expected from a percentage reduction of SO_2 emissions. This methodology relies on an intuitive mathematical approach that combines four separate effects: (1) the transport of atmospheric sulfur; (2) the possible nonlinearity of the SO_2-to-SO_4^{2-} chemical transformation; (3) the fraction of sulfates in fine particulate matter, taking into account the role of the water adsorbed by the fine particles; and (4) the fraction of light extinction that is due to fine particles. By looking at these four effects, within the context of each of the various meteorological regimes that have distinct influences on visual air quality, the problem can be broken down into manageable components that model a portion of the source–receptor interaction. If the necessary arrays that specify these four terms, which are expressed in fractional form, can be quantified for each region and meteorological classfication, then the methodology can estimate the average 'efficiency' of reductions in SO_2 emissions for producing improvements in long-term regional averages of visual range. Then, annual averages can be computed if the relative frequency of occurrence of each meteorological regime in each region is known. Moreover, the method estimates the uncertainty in the calculated percentage improvements in visual range, based on the uncertainties in input data. The second paper in this series will present an example of the application of this methodology to the eastern U.S., where the effect of SO_2 emissions on visibility has received significant attention.

Key word index: Atmospheric visibility, sulfur, emission controls, visibility modeling.

1. INTRODUCTION AND SUMMARY

Fine particles, i.e. particles whose diameter is less than 2.5 μm, are the most effective and important atmospheric component for visibility degradation. A large fraction of fine particles can be sulfate-containing particles, which are generated predominantly by atmospheric chemical reactions that oxidize gaseous SO_2, mostly emitted from anthropogenic sources, into sulfate particles (SO_4^{2-}). Several studies (e.g. Latimer and Hogo, 1987; EPA, 1988) have employed regional models in an attempt to quantify the role of SO_2 emissions on visibility impairment and to evaluate the visibility improvements that could be expected from SO_2 emission reduction scenarios. Such quantifications, however, are difficult to perform for several reasons: (1) the large uncertainties that even advanced models possess in simulating long-range transport, diffusion, chemistry and deposition of atmospheric sulfur; (2) the difficulty in quantifying the roles that other components, such as non-sulfate-containing fine particles, coarse particles and gases, play in visibility impairment (however, the upper limit of this contribution can often be quantified); and (3) the scarcity of suitable field data, with most measurement studies conducted during episodic conditions, while annual average assessments require input data that represent episodic as well as other conditions.

To circumvent the difficulties above, we have defined a semi-empirical approach that: (1) provides a straightforward solution to the problem; (2) accurately portrays the principal physical phenomena; (3) relies either on available data or, lacking 'hard' data, on expert judgment, and (4) takes into account the uncertainties in the input data. The method can be applied to different impact regions under different meteorological regimes and allows the computation of the visibility improvement in each region for each meteorological regime using an intuitive 'fractional' approach that is described quantitatively in the next section. The method represents the following premises.

(1) Atmospheric light extinction is caused by the concentration of fine particles and other airborne components. SO_2 emission controls will largely affect only the fraction of light extinction that is due to fine particles. (Actually, SO_2 controls will also affect sulfate-containing coarse particles, but with negligible associated visibility improvements.)

(2) The fine particle aerosol is composed of sulfate-containing particles and of particles containing other species (but no sulfates). SO_2 emission controls will affect only the fraction of the fine particles that contains sulfates. (Actually, SO_2 controls may increase the concentration of non-sulfate particles such as nitrate and chloride; see Pilinis (1990).)

(3) Fine sulfur-containing particles are a fraction of the total concentration of sulfur in the atmosphere in both gaseous and particulate form. They are produced mostly by SO_2-to-SO_4^{2-} chemical transformations that appear to be nonlinear. Therefore, although SO_2 emission controls will decrease proportionately the total ambient sulfur along the trajectories of plumes from controlled regions, the fine sulfates may decrease to a lesser extent because of the nonlinear chemistry.

(4) Total ambient sulfur in one geographical area is due to both local emissions and sulfur transported from other regions. SO_2 emission controls will affect only the fraction of sulfur that is transported from the regions affected by the control scenario.

In the rest of this paper we present the analytical description of our semi-empirical method (section 2), the definition of the input parameters (section 3), the calculation of the uncertainty in the results, based on the uncertainties on input data (section 4), and the conclusions (section 5). In the Appendix a discussion is provided on the problem of mathematically quantifying the economic benefits that can be expected from the calculated visual range improvements.

2. THE SEMI-EMPIRICAL METHOD

Let us define a control region $\mathscr{C}$, in which the fractional SO_2 control $\Delta E/E$ is to be implemented, where E is the total annual SO_2 emissions from the region $\mathscr{C}$ and ΔE (a negative number) is the total planned SO_2 emission reduction. Let us also define an impact region $\mathscr{I}$, where visual range improvements will be calculated, which is divided into suitable subregions ($j=1, 2, \ldots$) and whose meteorology can be classified into meteorological regimes ($k=1, 2, \ldots$). Each subregion should also be subdivided into an urban and a rural section, a differentiation that is useful since the sulfate fraction of the fine particles is larger in rural areas (Shea and Auer, 1978; Mathai and Tombach, 1985; Noll *et al.*, 1985) and the fraction of light extinction due to fine particles is generally lower in urban areas, where urban activities cause a relatively higher concentration of coarse particles. This regional division and meteorological classification allows the evaluation of the parameters required by the method, under the assumption that the properties of atmospheric diffusion and chemistry are similar during the days when the same meteorological scenario k occurs in the same region j.

We define as $(\Delta LE)_{jk}/(LE)_{jk}$ the average fractional improvement (a negative number) in light extinction in a subregion j during a day characterized by the k-th meteorological regime, where the light extinction LE (in units of 10^{-4} m^{-1}) is related to the visual range VR (in m) by

$$LE = 10^4 \cdot (3.0/VR) \tag{1}$$

where 3.0 is the value of the Koschmieder constant under the assumption of a human contrast perception threshold of 0.05 (Tombach and Allard, 1983).

Then the following identity can be written, where all the increments Δ are negative:

$$\underset{\text{I}}{\frac{(\Delta LE)_{jk}}{(LE)_{jk}}} \equiv \underset{\text{I}}{(\Delta E/E)} \; \underset{\text{II}}{\frac{\Delta E_j/E_j}{\Delta E/E}} \; \underset{\text{III}}{\frac{(\Delta S)_{jk}/(S)_{jk}}{\Delta E_j/E_j}} \; \underset{\text{IV}}{\frac{(\Delta SO_4)_{jk}/(SO_4)_{jk}}{(\Delta S)_{jk}/(S)_{jk}}} \; \underset{\text{V}}{\frac{(\Delta F^{(w)})_{jk}/(F^{(w)})_{jk}}{(\Delta SO_4)_{jk}/(SO_4)_{jk}}} \; \underset{\text{VI}}{\frac{(\Delta LE)_{jk}/(LE)_{jk}}{(\Delta F^{(w)})_{jk}/(F^{(w)})_{jk}}} . \tag{2}$$

Term I represents the average fractional SO_2 emission reduction throughout the control region $\mathscr{C}$. The term $(\Delta LE)_{jk}/(LE)_{jk}$, divided by Term I, gives the efficiency of SO_2 emission controls on light extinction; this efficiency will be written as $\theta_{jk}^{(w)}$ below. Term II is the ratio between the local fractional SO_2 control in the impact subregion j and the total average control in the region $\mathscr{C}$. It reflects the fact that the degree of control could differ from one region to the next and it is the only term in Equation 2 that can be greater than one. Term III is the ratio between the fractional improvement of total sulfur concentration, in the subregion j during the meteorological regime k, and the local fractional SO_2 control.

We indicate the product of Terms II and III by α_{jk}, which is the 'transport' efficiency of SO_2 emission controls on total sulfur concentrations and includes transport, diffusion and deposition phenomena. Therefore,

$$\frac{(\Delta S)_{jk}}{(S)_{jk}} = \alpha_{jk} \frac{\Delta E}{E}. \tag{3}$$

As will be seen in section 3.1, the term α_{jk} is less than unity in subregions j in which local and upwind fractional SO_2 emission controls are smaller than the average $\Delta E/E$. *Vice versa*, larger-than-average local and upwind controls generate values of α_{jk} greater than one.

Term IV is the ratio between the fractional improvement of the concentration of sulfate-containing particles (including associated cations) and the fractional improvement of the concentration of the total sulfur. This term, when less than unity, allows inclusion of nonlinearity of the SO_2-to-SO_4^{2-} reaction. Consideration of atmospheric chemistry needs to be included since numerical analyses (e.g. by Seigneur *et al.*, 1984) suggest that a given fractional decrease in ambient sulfur will generate a smaller fractional decrease of sulfate. We indicate this term as β_{jk}. Therefore,

$$\frac{(\Delta SO_4)_{jk}}{(SO_4)_{jk}} = \beta_{jk} \frac{(\Delta S)_{jk}}{(S)_{jk}}. \tag{4}$$

Term V is the ratio between the fractional improvement of the concentration of fine particles, including the water that they have adsorbed at ambient conditions, and the fractional improvement of the concentration of the sulfate particles (including associated cations but not including water). We indicate this term by $\gamma_{jk}^{(w)}$, where the superscript (w) emphasizes that the water adsorbed by the fine particles must be explicitly taken into account, as discussed in section 3.3, since this mass of water contributes to the total light extinction. Therefore,

$$\frac{(\Delta F^{(w)})_{jk}}{(F^{(w)})_{jk}} = \gamma_{jk}^{(w)} \frac{(\Delta SO_4)_{jk}}{(SO_4)_{jk}}. \quad (5)$$

The term $\gamma_{jk}^{(w)}$ is less than one, since $\gamma_{jk}^{(w)} = 1$ would indicate that all the fine particles are sulfate-containing particles.

Term VI is the ratio between the fractional improvement in light extinction and the fractional improvement of the concentration of fine particles (including water). We indicate this term by $\delta_{jk}^{(w)}$. Therefore,

$$\frac{(\Delta LE)_{jk}}{(LE)_{jk}} = \delta_{jk}^{(w)} \frac{(\Delta F^{(w)})_{jk}}{(F^{(w)})_{jk}} \quad (6)$$

which implicitly assumes that the different components of the fine particle concentration $F^{(w)}$ (i.e. sulfates, non-sulfate particles and water) have the same light extinction efficiency (extinction per unit mass of material). If necessary, however, this simplifying assumption can be removed, as discussed at the end of section 3.4. The term $\delta_{jk}^{(w)}$ is less than one, since fine particles are not the only cause of atmospheric light extinction.

By substituting Equations 3, 4, 5 and 6 into Equation 2, we obtain

$$\frac{(\Delta LE)_{jk}}{(LE)_{jk}} = \alpha_{jk}\, \beta_{jk}\, \gamma_{jk}^{(w)}\, \delta_{jk}^{(w)} \frac{\Delta E}{E} = \theta_{jk}^{(w)} \frac{\Delta E}{E} \quad (7)$$

where*

$$\theta_{jk}^{(w)} = \alpha_{jk}\, \beta_{jk}\, \gamma_{jk}^{(w)}\, \delta_{jk}^{(w)}. \quad (8)$$

The value $\theta_{jk}^{(w)}$ can be seen as the efficiency of the total SO_2 emissions control on light extinction, i.e. the percentage light extinction improvement for each region j and meteorological regime k, divided by the total percentage emission reduction in the region $\mathscr{C}$.

The calculation of the light extinction fractional improvements $(\Delta LE)_{jk}/(LE)_{jk}$ by Equation 7 allows the calculation of the visual range fractional improvements $I_{jk} = (\Delta VR)_{jk}/(VR)_{jk}$, which, from Equation 1, are

$$I_{jk} = \frac{(\Delta VR)_{jk}}{(VR)_{jk}} = -\frac{1}{1 + \dfrac{(LE)_{jk}}{(\Delta LE)_{jk}}} \quad (9)$$

These estimates of visibility improvements should not be construed as the improvements that could occur on any given day, but only those that would occur on the average during a meteorological regime k in the subregion j.

Finally, in each subregion j, the annual average fractional improvement I_j in visual range is

$$I_j = \sum_k p_{jk} I_{jk} \quad (10)$$

where p_{jk} is the relative frequency of occurrence of the meteorological regime k in the subregion j.

The fractional improvements of visual range computed above (i.e. I_{jk} and I_j), when divided by the average SO_2 fractional control $\Delta E/E$, provide the 'efficiencies' of SO_2 emission reduction on visual range. Once these efficiencies are computed for a certain SO_2 emission reduction scenario ΔE, they can be used, with some caution, to evaluate the visual range improvements of other SO_2 emission reduction scenarios that have spatial distribution and size similar to the original ΔE.

3. THE EVALUATION OF THE INPUT PARAMETERS

This section discusses the model parameters α_{jk}, β_{jk}, $\gamma_{jk}^{(w)}$, $\delta_{jk}^{(w)}$, and their physical significances, together with some illustrations of different ways of estimating them. The most reliable of these estimation techniques will be used in the application of the method in Part II of this two-part paper.

3.1. *The terms* α_{jk}

The efficiencies α_{jk} are defined by Equation 3 and can be estimated in several ways. For example, a simple estimate can be made using expert judgment†, through a subjective evaluation of the influences of the SO_2 emission control ΔE along the typical air mass trajectories under the different meteorological scenarios ($k = 1, 2, \ldots$). Ideally, for each subregion j and meteorological class k, typical backward trajectories could be plotted, thus allowing an expert to provide an approximate evaluation of the efficiency of a regional emission control on the total sulfur loading of that air mass. For example, if an air mass is passing through regions largely unaffected by the control ΔE, α_{jk} is much less than one, while if the air mass is dominated by the local emissions (e.g. during stagnant meteorological conditions), then $\alpha_{jk} \simeq (\Delta E_j/E_j)/(\Delta E/E)$ since Term III in Equation 2 is close to one. A more rigorous, and less subjective, evaluation of α_{jk} can be done using dispersion modeling techniques, which require, however, a reliable model and expensive

*Later in this paper, the product $\gamma_{jk}^{(w)}\, \delta_{jk}^{(w)}$ will be referred to as $\epsilon_{jk}^{(w)}$.

†We define expert judgment as an estimate of a physical parameter made by a professional expert in the field. The expert does not possess all the elements to perform a correct forecast, but is able, nevertheless, to provide an estimate based on previous, direct and indirect, experience. Clearly, large uncertainties are frequently associated with these estimates, which involves considerable subjectivity.

simulations of large, time-varying dispersion scenarios for a long period of time (e.g. 1 year).

We developed a simple 'intermediate' technique for evaluating α_{jk} that is not as subjective as the expert judgment discussed above and not as expensive as dispersion modeling. Let us define

$$(S)_{jk} = (S)^L_{jk} + (S)^D_{jk} \tag{11}$$

and

$$(\Delta S)_{jk} = (\Delta S)^L_{jk} + (\Delta S)^D_{jk} \tag{12}$$

where S indicates, as before, total sulfur concentrations, and the superscripts L and D indicate the contributions of the 'local' emissions (i.e. those from sources in the subregion j) and 'distant' emissions (i.e. those sources in regions upwind to the subregion j), respectively. Then, after some analytical manipulation in which we assume that total sulfur concentrations are proportional to the corresponding SO_2 emissions (e.g. $(\Delta S)^L_{jk}/(S)^L_{jk} = \Delta E_j/E_j$), we obtain

$$\frac{(\Delta S)_{jk}}{(S)_{jk}} = f^L_{jk}\frac{\Delta E_j}{E_j} + f^D_{jk}\frac{\Delta E_{j'(jk)}}{E_{j'(jk)}} \tag{13}$$

where

$$f^L_{jk} = (S)^L_{jk}/(S)_{jk} \tag{14}$$

$$f^D_{jk} = 1 - f^L_{jk} = (S)^D_{jk}/(S)_{jk} \tag{15}$$

and the region (or regions) j' is the area upwind of the subregion j during the meteorological regime k. Then, by substituting Equation 13 into Equation 3, we obtain

$$\alpha_{jk} = f^L_{jk}\frac{\Delta E_j/E_j}{\Delta E/E} + f^D_{jk}\frac{\Delta E_{j'(jk)}/E_{j'(jk)}}{\Delta E/E} = \alpha^L_{jk} + \alpha^D_{jk} \tag{16}$$

which can be interpreted as the sum of the 'local' term α^L_{jk} plus the 'distant' term α^D_{jk}.

The use of Equation 16 to evaluate α_{jk} requires identification of the 'upwind' region j' for each j and k and an assessment of the ratio $(S)^L_{jk}/(S)^D_{jk}$. As a first approximation that ratio can be set equal to 1, which means that total sulfur concentrations are due equally to local SO_2 sources (i.e. those in the same subregion j) and distant upwind sources. This assumption is not unreasonable, based on some studies (see, for example, Congress of the United States (1984)), but is, nevertheless, a major simplification of the complex phenomena of transport, diffusion and deposition of atmospheric sulfur.

Another difficulty is found when the 'upwind' region j' is outside the control region $\mathscr{C}$. Apparently, in this case, $\Delta E_{j'}/E_{j'}$ should be equal to zero. In reality, even though the control ΔE does not directly affect the region j', it could modify the background sulfur concentrations recirculating in the entire area. In other words, sulfur could be emitted in the region $\mathscr{C}$, transported into the region j' and then transported into the subregion j. In order to account for these recirculation effects, an appropriately non-zero value for $\Delta E_{j'}/E_{j'}$ should be used in these circumstances.

3.2. *The terms* β_{jk}

The terms β_{jk} are defined by Equation 4 and represent the linearity of the SO_2-to-SO_4^{2-} transformation. There is a disagreement in the scientific community about how much reduction in sulfate will result from a given percentage (say X) reduction in SO_2 emissions. The greatest SO_4^{2-} reduction percentage possible is X, assuming negligible primary emissions of sulfate particles and a totally linear relationship between SO_2 emissions and far downstream SO_4^{2-}. There are many indications, however, that there are conditions under which the conversion process is nonlinear, i.e. an X per cent reduction in SO_2 might result in a βX per cent reduction in SO_4^{2-}, with $\beta < 1$.

The technical arguments concerning SO_2 conversion are complex and the data needed to settle them are lacking. A mathematical simulation of reasonable chemical reactions for producing sulfate (Seigneur *et al.*, 1984) indicated that for $X = 50$ per cent in the eastern U.S., sulfate would decrease by $0.96X$ in a clear-sky environment in the summer and by $0.44X$ in a stratus-cloud environment in the summer. The implications are summarized by Latimer and Hogo (1987), who state "a 50 per cent reduction in SO_2 emissions may result in only a 30–40 per cent reduction in sulfate concentrations" and that "for now, the extent of nonlinearity remains a significant uncertainty" in calculations of sulfate reduction due to SO_2 emission reduction.

The simulations by Seigneur *et al.* can be used to estimate β_{jk} based on estimates of the cloudiness of each air mass k in each region j. Relatively cloud-free skies can be associated with $\beta_{jk} = 1$ (i.e. 'linear' chemistry), medium cloudiness with $\beta_{jk} = 0.85$, and extensive cloudiness with $\beta_{jk} = 0.70$.

3.3. *The terms* $\gamma^{(w)}_{jk}$

The terms $\gamma^{(w)}_{jk}$ are defined by Equation 5. It can be easily seen that

$$\gamma^{(w)}_{jk} = \frac{(SO^{(w)}_4)_{jk}}{(F^{(w)})_{jk}} \tag{17}$$

i.e. that $\gamma^{(w)}_{jk}$ is the sulfate fraction of fine particulates, including the contribution of the water. But aerosol measurements do not directly provide $\gamma^{(w)}_{jk}$, since fine particles are measured at a low relative humidity RH_0 (e.g. $RH_0 = 0.4$), where most of the water is removed from the particles collected on the ambient sampling filters. Measurements provide SO_4^{2-} (anion concentrations) and F (fine particle concentrations). Anion concentrations need to be multiplied by a factor λ, i.e.

$$SO_4 = \lambda SO_4^{2-} \tag{18}$$

in order to get the total mass concentration of the sulfate-containing component of particles. We assume that SO_2 controls do not affect the term λ. The value $\lambda = 1.25$, for example, can be used to represent a

particle mix* that is principally NH_4HSO_4 (acidic ammonium sulfate, for which $\lambda=1.20$) mixed with a little $(NH_4)_2SO_4$ (fully neutralized ammonium sulfate, with $\lambda=1.38$). Therefore, measurements can provide values of γ_{jk}, where

$$\gamma_{jk}=\frac{(SO_4)_{jk}}{(F)_{jk}}. \tag{19}$$

However, to estimate $\gamma_{jk}^{(w)}$ from γ_{jk}, assumptions need to be made about the amount of adsorbed water, as shown below.

Fine particles are the sum of sulfate (SO_4) and non-sulfate (NS) species. Therefore, we can write

$$F^{(w)}=SO_4^{(w)}+NS^{(w)}=K_s SO_4+K_{ns}\,NS \tag{20}$$

where K_s (a term greater than 1) represents a suitable 'amplification' of the SO_4 concentration to allow for the adsorbed water and, in a similar way, K_{ns} represents the increase for the concentration NS of non-sulfate particles. After some analytical manipulation we obtain

$$\gamma^{(w)}=\frac{\gamma}{\gamma+(1-\gamma)(K_{ns}/K_s)} \tag{21}$$

which correctly gives $\gamma^{(w)}=\gamma$ for $K_s=K_{ns}$ and $\gamma^{(w)}>\gamma$ for $K_s>K_{ns}$. The terms K_s and K_{ns} depend upon several factors, such as temperature, r.h. and pollutant concentrations. A simple approximation to evaluate them (Cass, 1979; Tang *et al.*, 1981; Appel *et al.*, 1985) gives

$$K_s=\left(\frac{1-RH_0}{1-RH}\right)^{\beta_s} \tag{22}$$

and

$$K_{ns}=\left[h_{ns}\left(\frac{1-RH_0}{1-RH}\right)^{\beta_{ns}}+(1-h_{ns})\right] \tag{23}$$

where RH is the ambient relative humidity, $RH_0\simeq 0.4$, h_{ns} is the fraction of NS that is hygroscopic, and β_s, β_{ns} are exponents that need to be evaluated ($\beta=1$ or 2 have often been chosen).

More complex modeling techniques can be used to calculate more precise values of K_s and K_{ns}. For example, Pilinis and Seinfeld (1987) developed and tested a computer code that performs a chemical equilibrium calculation in the sulfate, nitrate, chloride, sodium, ammonium and water system. This computer code was successful in predicting the concentrations of various aerosol species at Long Beach, California. Its application, however, requires detailed air quality and meteorological information that is often unavailable on a regional and annual average basis. Hence, there is the need to use, at least at the present time, semi-empirical relations such as Equations 22 and 23.

* This example of mix is consistent with the findings of the Sulfate Regional Experiment (Muller and Hidy, 1983).

3.4. *The terms* $\delta_{jk}^{(w)}$

The terms $\delta_{jk}^{(w)}$ are defined by Equation 6. They represent the fraction of light extinction that is attributable to fine particles at ambient conditions. The light extinction can be written as

$$LE=e_f F^{(w)}+LE_0 \tag{24}$$

where e_f is the light extinction efficiency of the fine particulate matter, including water, and is typically in the range of 3–4 $m^{-1}\,g^{-1}\,m^{-3}$ (or $3–4\times10^{-2}$, if LE is in $10^{-4}\,m^{-1}$ and $F^{(w)}$ in $\mu g\,m^{-3}$), where (contrary to normal practice) the mass includes the mass of water. LE_0 is the light extinction that is not caused by fine particles, e.g. Rayleigh scattering by air, absorption by NO_2 gas, and scattering and absorption by coarse particles.

From Equation 24 we obtain

$$\delta_{jk}^{(w)}=\frac{e_f(F^{(w)})_{jk}}{(LE)_{jk}} \tag{25}$$

which is difficult to evaluate from available measurements. LE can be computed from measurements of the visual range VR (e.g. made at airports), using Equation 1; and $F^{(w)}$ can be computed by

$$F^{(w)}=\left(\frac{1-RH_0}{1-RH}\right)^{\beta_f}F \tag{26}$$

where the F values are obtained from aerosol measurements (which remove most of the water) and the exponent β_f needs to be evaluated (e.g. $\beta_f=1$).

The δ values can also be evaluated using a site-specific extinction efficiency, instead of a literature value of e_f. It suitable measurements of VR and F are available in the subregion j, then, for each set of days characterized by a meteorological regime k, LE can be computed from Equation 1 and $F^{(w)}$ from Equation 26. Then, the linear regression

$$(LE)_{jk}=a_{jk}(F^{(w)})_{jk}+b_{jk} \tag{27}$$

can be performed, which provides the coefficients a_{jk} and b_{jk} that allow the calculation of $\delta_{jk}^{(w)}$ as

$$\delta_{jk}^{(w)}=\frac{a_{jk}}{a_{jk}+b_{jk}/(F^{(w)})_{jk}}. \tag{28}$$

This correctly gives $\delta_{jk}^{(w)}=1$ for $b_{jk}=0$. Regression results, however, must be used with caution since they can sometimes be misleading and, therefore, require careful analysis and interpretation.

The terms $\gamma^{(w)}$ and $\delta^{(w)}$ can also be combined. If we define $\epsilon^{(w)}=\gamma^{(w)}\delta^{(w)}$, then

$$\frac{(\Delta LE)_{jk}}{(LE)_{jk}}=\epsilon_{jk}^{(w)}\frac{(\Delta SO_4)_{jk}}{(SO_4)_{jk}}. \tag{29}$$

This new notation allows, if necessary, a differentiation between sulfate and non-sulfate light extinction efficiency, instead of using the efficiency e_f for both as previously done in Equation 24. In fact, light extinc-

tion can be written as

$$LE = 10^4 \frac{3.0}{VR}$$

$$= e_s^{(w)} SO_4 + e_{ns}^{(w)} NS + LE_0$$

$$= e_s^{(w)} \lambda\, SO_4^{2-} + e_{ns}^{(w)} (F - \lambda\, SO_4^{2-}) + LE_0 \quad (30)$$

where

$$e_s^{(w)} = e_s + e_w(K_s - 1) \quad (31)$$

$$e_{ns}^{(w)} = e_{ns} + e_w(K_{ns} - 1)h_{ns} \quad (32)$$

and e_s, e_{ns}, e_w are the extinction efficiencies of sulfate, non-sulfate and water, respectively. Then, we obtain

$$\epsilon^{(w)} = \frac{e_s^{(w)}}{e_s^{(w)} + e_{ns}^{(w)} \dfrac{1-\gamma}{\gamma} + \dfrac{LE_0}{\gamma F}}. \quad (33)$$

If suitable measurements of VR, SO_4^{2-}, and F are available, for each set of days in the subregion j characterized by a meteorological regime k, we can perform a new linear regression, based on Equation 30 instead of Equation 27, which provides $(e_s^{(w)})_{jk}$, $(e_{ns}^{(w)})_{jk}$ and $(LE_0)_{jk}$, and therefore, allows a site-specific evaluation of $\epsilon_{jk}^{(w)}$ from Equation 33.

4. UNCERTAINTY ANALYSIS

Actual application of the methodology presented above should be associated with an analysis of the uncertainty in the results. As a result of uncertainties in all the variables, there is no unique answer for the visibility improvement I_{jk} for a given $\Delta E/E$, but rather there is a range of possible improvements with associated probabilities. This section reviews the methods used to calculate a probability distribution for visual range improvements as computed by Equations 7 and 9. This probability distribution can be calculated by obtaining probability distributions for the input variables (to reflect their uncertainties) and combining these distributions. The input probability distributions are constructed separately for each of the four input variables (α_{jk}, β_{jk}, $\gamma_{jk}^{(w)}$, $\delta_{jk}^{(w)}$) described previously, for each subregion, j, and meteorological regime, k.

The unconditional distribution for I_{jk} is computed by integrating over the probability of the visual range improvement (given a ΔE and the four factors) multiplied by the joint distribution of the four factors, i.e.

$$p(I_{jk}|\Delta E) = \int_\alpha \int_\beta \int_\gamma \int_\delta p(I_{jk}|\Delta E, \alpha_{jk}, \beta_{jk}, \gamma_{jk}^{(w)}, \delta_{jk}^{(w)})\, p(\alpha_{jk}, \beta_{jk}, \gamma_{jk}^{(w)}, \delta_{jk}^{(w)}). \quad (34)$$

In this equation, we use the notation $\int_\alpha$ to be the generalized summation symbol, which is interpreted as summation when α is discrete and integration when α is continuous.

The joint probability distribution for all four factors is equal to the product of their individual probability distributions if we make the reasonable assumption that their distributions are mutually independent, i.e.

$$p(\alpha_{jk}, \beta_{jk}, \gamma_{jk}^{(w)}, \delta_{jk}^{(w)}) = p(\alpha_{jk})\, p(\beta_{jk})\, p(\gamma_{jk}^{(w)})\, p(\delta_{jk}^{(w)}). \quad (35)$$

A similar discussion applies to the annual fractional visual range improvements, I_j. From Equation 9 we obtain, by assuming that p_{jk} are exactly known, that the conditional probability distribution for I_j is

$$p(I_j|\Delta E, \alpha_{j.}, \beta_{j.}, \gamma_{j.}^{(w)}, \delta_{j.}^{(w)}) = \int_k p(I_{jk}|\alpha_{jk}, \beta_{jk}, \gamma_{jk}^{(w)}, \delta_{jk}^{(w)})\, p_{jk} \quad (36)$$

and the unconditional distribution is

$$p(I_j|\Delta E) = \int_\alpha \int_\beta \int_\gamma \int_\delta \int_k p(I_{jk}|\alpha_{jk}, \beta_{jk}, \gamma_{jk}^{(w)}, \delta_{jk}^{(w)})\, p_{jk}\, p(\alpha_{jk}, \beta_{jk}, \gamma_{jk}^{(w)}\, \delta_{jk}^{(w)}) \quad (37)$$

where the notation $j.$ indicates the set $j1, j2, \ldots$.

In this paper, we suggest the use of a probability tree to construct the distributions of interest, i.e. $p(I_{jk}|\Delta E)$ and $p(I_j|\Delta E)$, from $p(\alpha_{jk})$, $p(\beta_{jk})$, $p(\gamma_{jk}^{(w)})$ and $p(\delta_{jk}^{(w)})$. We choose this approach because it is straightforward and affords us the opportunity to trace specific scenarios through the probability tree. Thus, the specific calculations we performed can be exactly replicated rather than relying on the randomized procedure of Monte Carlo techniques. We use a probability tree by choosing, from each input variable's probability distribution, three predetermined points from which to construct our scenarios. These points and their associated probabilities are chosen in a manner that exactly preserves the mean, variance, skewness, and kurtosis of the original distributions. The reader is referred to the paper of Miller and Rice (1983) for more discussion of this probability tree method. For example, in the case of normal distributions, we should use three probability-value pairs defined as:

Probability	Value
1/6	Mean − 1.7 × standard deviation
2/3	Mean
1/6	Mean − 1.7 × standard deviation

Distributions other than the normal distribution have analogous theoretical results. The predetermined points shown above apply only to normal distributions.

Using this method, the resulting probability tree contains 3^4 or 81 scenarios, which allow the approximation of the probability distribution for visual range improvements described in Equation 34 by a stepwise function of 81 values. An example of application of the probability tree methodology discussed above is presented in the Part II of this paper.

5. CONCLUSIONS

We have presented a semi-empirical methodology for evaluating the visibility improvements that can be expected in an impact region $\mathscr{I}$ from SO_2 emission reduction scenarios in a control region $\mathscr{C}$. We have also discussed the problems associated with the evaluation of model parameters and the uncertainty of the results. Finally, in the Appendix, we show how the results of our semi-empirical method could be used to evaluate the dollar benefits associated with the visibility improvements.

The proposed semi-empirical methodology is conceptually simple. Its parameters can be estimated from the analysis of measurement data and the use of expert judgment. Alternatively, modeling techniques can be used to estimate α (dispersion models), β (chemical models), $\gamma^{(w)}$ (models that simulate the adsorption of water by atmospheric fine particles) and $\delta^{(w)}$ (light extinction model).

The second paper of this two-paper series will provide an example of an application of this technique (without quantification of economic benefits, though) to the eastern U.S., where SO_2 emissions have been the main focus of attention for visibility degradation.

Acknowledgements—We thank Dr Prem Bhardwaja (Salt River Project) for his critical review and Dr William Wilson (U.S. EPA) for suggesting the explicit treatment of the role of water. We extend our appreciation to Ms Wendy Webb for typing the manuscript and to Ms Anita Spiess for editorial review. This study was sponsored by the Utility Air Regulatory Group (UARG).

REFERENCES

Appel B. R., Tokiwa Y., Hsu J., Kothny E. L. and Hahn E. (1985) Visibility as related to atmospheric aerosol constituents. *Atmospheric Environment* **19**, 1525–1534.

Cass G. R. (1979) On the relationship between sulfate in air quality and visibility with examples in Los Angeles. *Atmospheric Environment* **13**, 1069–1084.

Congress of the United States (1984) Acid rain and transported air pollutants—implications for public policy. Office of Technology Assessment document OTA-0-204.

Horvath H., Gorraiz J. and Raimann G. (1986) On the importance of color contrasts for the visibility of targets and for the recognition of targets at distances smaller than the visual range. Presented to the Air Pollution Control Association, September.

Latimer D. A. and Hogo H. (1987) The relationship between SO_2 emissions and regional visibility in the eastern United States. APCA Specialty Conference, Visibility Protection: Research and Policy Aspects. Grand Teton National Park, Wyoming, September 1986.

Malm W. (1985a) An examination of the ability of various physical indicators to predict judtement of visual air quality. Presented at Air Pollution Control Association, 16 June.

Malm W. (1985b) Assessment of visibility impairment on visitor enjoyment and utilization of park resources. CIRA, Colorado State University, March.

Mathai C. V. and Tombach I. H. (1985) Assessment of the technical basis regarding regional haze and visibility impairment. AeroVironment Report AV-FR-84/420, Monrovia, California.

Miller A. and Rice T. (1983) Discrete approximations of probability distributions. *Manag. Sci.* **29**, 352.

Mueller P. K. and Hidy G. M. (1983) The Sulfate Regional Experiment: Report of findings. Electric Power Research Institute, Report EA-1901, Palo Alto, California.

Noll K. E., Pontius A., Frey R. and Gould M. (1985) Comparison of atmospheric coarse particles at an urban and nonurban site. *Atmospheric Environment* **19**, 1931–1943.

Pilinis C. (1990) Numerical simulation of visibility degradation due to particulate matter: model development and evaluation. *J. geophys. Res.* (submitted).

Pilinis C. and Seinfeld J. H. (1987) Continued development of a general equilibrium model for inorganic multicomponent atmospheric aerosols. *Atmospheric Environment* **21**, 2453–2466.

Ruud P. A. (1985) A review of the SAI report to EPA. Report prepared for the Utility Air Regulatory Group (1985). See also Ruud P. A. and Balson W. E. (1987) Assessment of household values for visual range improvements. 81st APCA Annual Meeting, Dallas, Texas. Paper 88–56.12.

Seigneur C., Saxena P. and Roth P. M. (1984) Computer simulations of the atmospheric chemistry of sulfate and nitrate formation. *Science* **225**, 1028–1030.

Shea D. M. and Auer A. H., Jr. (1978) Thermodynamic properties and aerosol patterns in the plume downwind of St. Louis. *J. appl. Met.* **17**, 689–698.

Stewart T., Middleton P. and Ely D. (1983) Urban visual air quality judgments: Reliability and validity. *J. Envir. Psychol.* **3**, 129–145.

Systems Applications, Inc. (1984) Visibility and other air quality benefits of sulfur dioxide emission controls in the eastern United States. Draft report SYSAPP-84/165.

Tang I. N., Wong W. T. and Munkelwitz H. R. (1981) The relative importance of atmospheric sulfates and nitrates in visibility reduction. *Atmospheric Environment* **15**, 2463–2471.

Tombach I. and Allard D. (1983) Comparison of visibility measurement techniques: Eastern United States. Electric Power Research Institute Report EA-3292, Palo Alto, California.

United States Environmental Protection Agency (1988) Regulatory impact analysis on the national ambient air quality standards for sulfur oxides (sulfur dioxide). Draft report prepared by the Air Quality Management Division, Office of Air and Radiation, U.S. EPA, Research Triangle Park, North Carolina (March, 1988).

APPENDIX: THE QUANTIFICATION OF ECONOMIC BENEFITS

Even though visibility impairment can be expressed by several factors (e.g. changes in contrast, discoloration, reduction of visual range, etc.), the lack of data has restricted most

visibility studies to the analysis of the visual range, a parameter that is routinely measured at airports. For this reason, visual range has become the attribute of visibility with which policy makers are most concerned (SAI, 1984; EPA, 1988).

Improvements in visual range can be associated with economic benefits in several ways (EPA, 1988). One common approach involves the calculation of the average household 'willingness to pay'* for a fractional visibility improvement

$$I=\Delta VR/VR. \tag{A1}$$

More precisely, a $\Delta\$(\Delta E)$ can be defined as the total annual benefit, in the impact region $\mathscr{S}$, associated with the visual improvements from the SO_2 emission control ΔE, where

$$\Delta\$(\Delta E)=\sum_j \frac{P_j}{A_j}\sum_k p_{jk} H_{jk}(\Delta E). \tag{A2}$$

In Equation A2, P_j is the number of people living in the subregion j, A_j is the average household size†, p_{jk} is the relative frequency of occurrence of the meteorological regime k in the subregion j, and $H_{jk}(\Delta E)$ is the average annual willingness per household in the subregion j to pay for the visibility improvement I_{jk} achieved by the control ΔE under the kth meteorological regime. It is important to note that, in Equation A2, the summation over k should not include meteorological scenarios that produce a strong visibility reduction as a consequence of natural phenomena (e.g. cases in which the r.h. is greater than 85%). In these circumstances, the visibility benefits of the SO_2 reduction are virtually undetectable by the human observer.

Two factors make Equation A2 more complicated than it looks. First, our semi-empirical method provides improvements I_{jk} that are averages for the time that the meteorological regime k occurs in the subregion j. The actual daily values of I will vary according to a probability density function that we indicate by $p(I_{jk}^{(d)})$, where the superscript (d) emphasizes that this probability function describes the daily variation of I, while $p(I_{jk}|\Delta E)$ in section 4 represents the probability distribution of the average visual range improvements I_{jk}. Second, no benefit should be allocated for improvements I that are undetectable‡ by the population P_j. We know that an improvement I cannot be detected when it is below a threshold value I^*. We also know that different people have different thresholds. Therefore, we can assume, in total generality, that the threshold value I^* varies among the population P_j with a probability density function $p(I^*)$. If we take these two factors into account, we obtain

$$H_{jk}(\Delta E)=\int_0^{+\infty} p(I_{jk}^{(d)}) \int_0^I H_j(I, I^*)p(I^*)\mathrm{d}I^*\,\mathrm{d}I \tag{A3}$$

where $H_j(I, I^*)$ is the household willingness to pay in the subregion j for a fractional visibility improvement I with a threshold I^*. Note that, in Equation A3, I is always greater than I^*. Several different functions can be used for $H_j(I, I^*)$. For example, SAI (1984), in the eastern U.S., used a logarithmic relation (see Fig. A-1)

$$H_j(I, I^*)=b\ln(1+I) \quad \text{for } I\geqslant I^*$$
$$H_j(I, I^*)=0 \quad \text{for } I<I^* \tag{A4}$$

with b in the range between \$133.67 and \$473.07, and a mid-range value equal to \$243.03. A lower value (b=\$90.30) was proposed by Ruud (1985). It seems unrealistic, however, to represent $H_j(I, I^*)$ by a step function at the threshold value I^*, since a smooth increase in value from $H_j=0$ at $I=I^*$ is more likely to occur. We believe that different functions for $I\geqslant I^*$ should be used, such as the logarithmic relation

$$H_j(I, I^*)=b_j\ln\left(1+\frac{I-I^*}{1-I^*}\right) \tag{A5}$$

or the linear relation

$$H_j(I, I^*)=b_j\frac{I-I^*}{1-I^*}\ln 2 \tag{A6}$$

both outlined in Fig. A-1.

The combination of Equations A2 and A3, with a suitable choice of $H_j(I, I^*)$, gives the total annual dollar benefit. This calculation is a convolution of three probability density functions: p_{jk}, $p(I^*)$ and $p(I_{jk}^{(d)})$. The first, p_{jk}, can be obtained from measurements and meteorological classification. The second, $p(I^*)$, can be assumed to have a log-normal distribution, with 95% of the people in the range $I^*=0.07$ and $I^*=0.29$. These two extreme values correspond to contrast change thresholds $\Delta C^*=0.02$ and $\Delta C^*=0.10$, and were calculated using a formulation presented by SAI (1984), assuming the Koschmieder constant (the constant in Equation 1) equal to 3.0, the ratio of the object distance from constant (the constant in Equation 1) equal to 3.0, the ratio of the object distance from the observer to the visual range equal to 0.33, and the intrinsic contrast of the landscape feature equal to -0.8. It can be found that the above assumptions for $p(I^*)$ correspond to

$$p(\ln I^*)=N(0.143, 0.335) \tag{A7}$$

where $N(\mu, \sigma)$ indicates the normal (Gaussian) distribution with average μ and standard deviation σ.

The third probability density function, $p(I_{jk}^{(d)})$, is difficult to evaluate. Our semi-empirical method provides estimates of the averages I_{jk}, and their probability distribution $p(I_{jk}|\Delta E)$, but does not provide the daily statistical distributions $p(I_{jk}^{(d)})$ of the visual improvements I. Further assumptions, therefore, need to be made for computing the benefits. For example, as a first approximation, we can assume $p(I_{jk}^{(d)})=p(I_{jk}|\Delta E)$, even though the two probability functions are conceptually different.

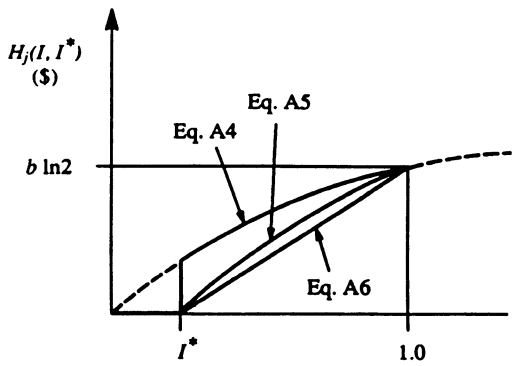

Fig. A-1. Three alternate representatives of a bid function $H_j(I, I^*)$ that reflect the effect of a threshold I^* for the fractional visibility improvement I.

* This approach ignores, however, the preservation values.

† For example, a constant value of $A_j=2.72$ was used by SAI (1984) in the eastern U.S.

‡ Active research programs have been sponsored by the U.S. EPA, the National Park Service (NPS), and the Electric Power Research Institute (EPRI) that focus primarily on the psychophysical response of the eye–brain system to changes in the attributes of visibility. This psychophysical research is intended to determine an effective visibility index by which to measure perceptible changes in visibility. (Malm, 1985a, b; Stewart, 1983; Horvath, 1986.)